Systems & Control Transactions

Original Research Article: Revised Version
Peer Reviewed Conference Proceeding
ESCAPE 36 - European Symposium on Computer Aided Process Engineering
Sheffield, UK. 21-24 June 2026

PSE PRESS

High Performance Heat Pumps Using Tailored Refrigerants

Finlay M. Sandham, Andrew Muumbo, Kenneth Mathew, Sarthak Sinha and Smitha Gopinath*

University of Sheffield, School of Chemical, Materials, & Biological Engineering, Sheffield, United Kingdom
* Corresponding Author: s.gopinath@sheffield.ac.uk

ABSTRACT

Heat Pumps (HPs) can play a vital role in the decarbonization of heating in industry. The performance of a HP strongly depends on the refrigerant, the working fluid within the HP. In order to maximize HP performance, systematic selection of the refrigerant is key. Refrigerant choice affects the very feasibility of employing a HP to deliver heating to a process. A flexible and robust method is required to select refrigerants that are the best fit for a given heating application. A computer-aided molecular & process design (CAMPD) method is developed to design the optimal refrigerant that is tailored to process needs. The method is applied to three case studies across which the HP performance objectives and constraints, and heat source and heat sink temperatures are varied. In addition, the design of refrigerants with low (<150) global warming potentials and zero ozone depletion potentials is investigated. For all applications across all case studies, the CAMPD approach successfully identifies high-performance refrigerants including those that are known refrigerants, other known fluids and novel molecules.

Keywords: optimization, molecular design, decarbonization, process design

INTRODUCTION

Heat consumption in industries worldwide is around 110 EJ per year [1]. Over 90% of this heat is generated by the combustion of fossil fuels, resulting in 21% of global carbon dioxide emissions [2]. Heat pumps (HPs) that are powered by electrical energy and offer high energy efficiencies are a promising alternative heating solution. HPs harness heat from a low-temperature heat source and upgrade it to an increased, useful temperature by utilizing (electro-)mechanical work. HPs are able to utilize both ambient heat and waste heat due to which the work input into the HP is only a fraction of the heat they supply. HPs can be driven by low-emissions electricity, yielding low-carbon heating.

The working fluid within the HP is known as the refrigerant. HPs based on the subcritical vapour compression cycle are the focus of this work. In the evaporator of the HP, the low-pressure refrigerant takes up thermal energy from a (low temperature) heat source, at temperature T_{source}, and vaporizes. The gaseous refrigerant is compressed to a higher pressure and temperature in the compressor. In the condenser, the high-temperature refrigerant releases thermal energy to the heat sink, which is at temperature T_{sink}, and condenses. To complete the cycle, the refrigerant passes through the expansion valve (sometimes called a throttling valve) that causes a drop in pressure and temperature. This process is illustrated in figure 1.

The application of HPs in the process industries necessitates innovation in the design of HPs. HPs may be used to deliver heating to a variety of unit operations such as distillation columns, dryers, and reactors whose temperatures are below 200 °C [3]. At the same time, several (waste) heat sources whose temperature vary between 30 °C and 200 °C are available in the process industries [3]. Given the large number of heat sources and sinks and the diversity of their temperatures and heat duties, HPs and their refrigerants need to be tailored to each application to maximize performance. The refrigerant in the HP must satisfy manifold requirements: (i) the refrigerant must be able to undergo phase transitions in both the evaporator and condenser; ii) the boiling point of the refrigerant in the evaporator must be below T_{source} at pressures above 1 atm (to prevent vacuum operations); iii) the critical temperature of the

refrigerant must be higher than T_{sink} to allow the refrigerant to deliver heat by condensation; and iv) the refrigerant must be compatible with compressor seals and lubricant.

Apart from the performance of the refrigerant in the HP, there are several environmental and safety-related implications to the choice of the refrigerant. Refrigerants containing chlorine can have high ozone depletion potentials (ODPs) and have been phased out by the Montreal protocol [4]. They have been replaced by fluorinated refrigerants, many but not all of which have very high global warming potentials (GWPs), exceeding the regulatory limit of 150 [5]. Several fluorinated molecules are either expected to be phased out or are already banned due to their high GWPs, toxic degradation products, and pervasiveness in the environment [5]. Natural refrigerants, which include molecules such as alkanes, alkenes, and ammonia, are a promising alternative class of refrigerants. However, several of these are highly flammable, restricting their use across settings. Water and carbon dioxide are non-flammable natural refrigerants that offer high safety and good performance for a limited range of temperatures.

Given the shortcomings of known refrigerants, the discovery of new refrigerants is essential. Further, it is crucial to systematically select the best-fit refrigerant considering both process-specific needs (heat duties, temperatures) as well as the availability of waste heat streams (heat capacities and temperatures). In addition, the refrigerant must comply with environmental and safety-related regulations, e.g., the GWP of the refrigerant must be lower than the legal limit.

Most previous computational techniques for refrigerant selection use a screening process, where all molecules within a chemical database are examined to find those with desirable properties or performance. Examples of such studies include [6], [7], [8].

Computer-aided molecular & process design (CAMPD) is an alternative that can be used to identify best-fit refrigerants. In this framework, an optimization problem is formulated to find the optimal refrigerant and process conditions of the HP. [9] Applied CAMPD to find refrigerant candidates for a domestic HP using detailed process models including a sophisticated compressor model.

In this work we simultaneously find the refrigerant and the process variables that satisfy performance constraints and maximize the thermodynamic performance of a subcritical vapor-compression industrial HP, using a CAMPD approach. The best possible pure-component refrigerant, be it a known refrigerant, other known fluid, or a novel molecule, is identified from within a large molecular design space. To the best of our knowledge, this is the first CAMPD study on the basis of rigorous thermodynamic models that is applied to high-temperature industrial HPs and that also considers the environmental properties of the refrigerant. In this work, we systematically investigate the use of CAMPD to design HPs by i) varying heat source and heat sink temperatures; ii) varying HP performance objectives; and iii) restricting refrigerants to be low-GWP and zero-ODP. We also benchmark the performance of designed refrigerants against known refrigerants to study the effectiveness of this CAMPD approach.

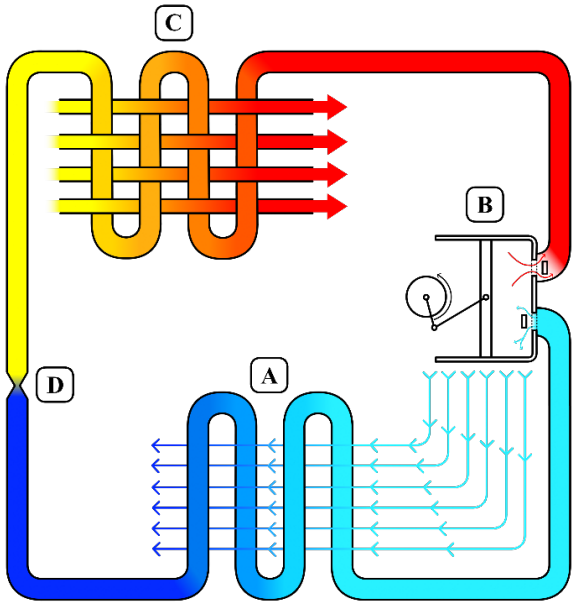

Figure 1. A diagram of a vapor-compression HP cycle. A: Evaporator; B: Compressor; C: Condenser; D: Expansion valve

CAMPD OF HP

The HP cycle is modelled in gPROMS Process 2024.1.0 using MESH (Mass, Equilibrium, Summation, and Enthalpy) models. These models do not consider sizing or costing of HP equipment. Several assumptions are made in modelling the HP. The heat source and heat sink are isothermal reservoirs at temperatures T_{source} and T_{sink}, respectively. The evaporator and condenser are isobaric at pressures P_{evap} and P_{cond}, respectively. The compressor has an isentropic efficiency of 70%, and the motor and drivetrain have a combined efficiency of 95%. The expansion valve is isenthalpic. There are no pressure drops or heat losses in the connections between unit operations.

The performance of the HP cycle is quantified using two metrics: coefficient of performance (COP) and volumetric heating capacity (VHC). The COP, a measure of energy efficiency, is the ratio of heat delivered to the heat sink (Q_{out}) to compressor power consumption (W_{in}). The VHC is the energy delivered to the heat sink per unit volume of refrigerant at the compressor inlet ($V_{comp.inlet}$),

i.e., $VHC = \frac{Q_{out}}{V_{comp.inlet}}$. VHC is indicative of the sizing of the HP. The temperature lift ΔT_{lift} of the HP is given by $\Delta T_{lift} = T_{sink} - T_{source}$.

Process-Level Degrees of Freedom.

In the optimization of this HP model, the following process-level degrees of freedom are considered as continuous decision variables:

The condenser pressure P_{cond}

The condenser subcool ΔT_{sub}

The evaporator pressure P_{evap}

The evaporator superheat ΔT_{super}

In addition, the chemical composition of the refrigerant is a decision variable. The refrigerant is represented using a vector of integers $\boldsymbol{n}$, where each element of the vector n_i represents the number of occurrences of functional/atomic group i in the refrigerant. For example, to represent butanol, the vector elements corresponding to -OH, -CH_2-, and -CH_3 would be set to 1, 3, and 1, respectively, and all other elements of $\boldsymbol{n}$ would be set to 0. 20 chemical groups are allowed in the refrigerant, as outlined in Table 1. Up to 10 occurrences of each group are allowed in the molecule, other than >N- which can take a maximum value of 1 to avoid complex branching structures. The group -cO- refers to an oxygen atom that is attached to two -CH_2- groups, and the -eO- group is an (end) ether group in which the oxygen atom is connected to a -CH_3 group.

Table 1: The groups considered in the CAMPD problem.

Chemical family	Groups
Hydrocarbons	-CH_2-, -CH_3,
Olefins	=CH_2, =CH-
Alcohols, carboxylic acids	-OH, -eO-,
ethers, esters, and ketones	-cO-, >C=O, -COO, -COOH
Chlorocarbons	-$CHCl_2$, -CH_2Cl
Fluorocarbons	-CF_3 -CHF_2, -CH_2F, -CF_2-, -CHF-
Amines	-NH_2, -NH-, >N-

Group contribution methods (GCMs)

Group contribution methods (GCMs) are used to estimate physicochemical properties of the refrigerant, which is described by its chemical composition vector $\boldsymbol{n}$. The group contribution equation of state (EoS) SAFT-γ Mie [10] is used to predict the thermodynamic properties of the refrigerant molecule both as a function of $\boldsymbol{n}$ and its state (temperature, pressure) in the process. SAFT-γ Mie was chosen for its accuracy in predicting both calorific properties and vapour-liquid equilibria, its ability to describe a wide range of refrigerants and fluids, and its proven use in similar CAMPD problems [11]. The SAFT-γ Mie EoS is included in the inbuilt gProperties tool in gPROMS Process, which is used to compute thermodynamic properties. The parameters for the fluorinated groups are taken from Martínez [12] and all others are taken from the gProperties databank.

While the SAFT-γ Mie EoS can predict all thermodynamic properties of fluids, the accuracy of critical point predictions is typically low. Thus, a first-order semi-empirical group contribution model was chosen to model the critical point. [13] was chosen for its higher accuracy in comparison to two other methods [14], [15] for a small test of molecules.

The work of [16] is used for GWP prediction. Again, only first-order group contributions are considered. For groups with no computed GWP contribution, such as -CH_2-, the contribution is assumed to be negligible and is set to 0. However, this approach did not account for the significantly reduced GWP of molecules with double bonds - the atmospheric lifespan of these molecules is greatly reduced which causes them to have a lower GWP. Therefore, we parameterized first-order contributions for =CH- and =CH_2 groups by regressing to GWP data from [17]. The contribution calculated for =CH- is -1.618305, and for =CH_2 is -0.502935.

Objectives & Constraints

The CAMPD problem is formulated to maximize one of two objective functions: COP, and VHC. The design problem is subject to process-related constraints to ensure feasible operation of the subcritical HP cycle. Molecular feasibility constraints are added to ensure that the octet rule is satisfied for all atoms in the molecule. Several new molecular feasibility constraints are introduced to prevent molecules that are known to be unstable stable such as geminal diols, geminal amines, α-haloalcohols, peroxides and peracids. Further, for molecules that exhibit keto-enol and amine-imine tautomerism, the enol and amine forms that are typically unstable in aliphatic molecules are excluded. The process constraints and molecular feasibility constraints are listed in the supplementary information (SI).

Experiments

The full MINLP is implemented in gPROMS Process 2024.1.0 using gProperties v2.8 and solved using the MINLPOA solver which is based on the outer approximation algorithm [25] with equality relaxation and augmented penalty. This algorithm works by sequentially solving a primal continuous nonlinear program (NLP) and a master mixed-integer linear program (MILP). The NLP is solved using the NLPSQP algorithm.

Only local optima of this non-convex problem are obtained by solving the MINLP. To obtain high-quality

solutions, integer cuts are used to re-solve each design problem while excluding previous solutions. The integer cut is as is shown in Equation 1 ([18], [19]), where $\boldsymbol{p}$ is a vector of the first 20 prime numbers, M is a sufficiently large number, 10,000 for this problem, $\boldsymbol{n}^{cut}$ is the solution to be excluded, y is a binary decision variable, and ϵ is a tolerance, which is set to 2 in this case.

$$My + \epsilon < \boldsymbol{p}^T\boldsymbol{n}^{cut} - \boldsymbol{p}^T\boldsymbol{n} < M(1-y) - \epsilon \quad (1)$$

Computational experiments are performed to observe how the solution changes across different source-sink temperatures, design objectives, and constraints. The experiments are run from source temperatures of 340 K to 420 K and sink temperatures of 360 K to 440 K at temperature intervals of 20 K. For each source-sink temperature pair, the MINLP optimization is solved 4 times using 3 successive integer cuts to generate 4 different candidate solutions. The best-found solution found over the 4 runs is then reported for each temperature pair. The initial guess for all MINLP solves is fixed and given in the SI. In order to facilitate these experiments a computer program was developed in C++ to call gPROMS optimizations through the gO:RUN feature at the specified source-sink temperatures and to automatically apply the integer cuts.

Table 2: Summary of experiments

Case	Objective	Additional Restrictions
1	VHC	None
2	COP	None
3	COP	Constraint on GWP (<150 as per EU F-gas regulations), zero ODP enforced by removal of chlorine containing groups. Restricted design space through removal of nitrogenated and fluorinated groups.

The results are benchmarked against four existing refrigerants that are already being used in HPs [20]. The benchmark refrigerants are ammonia (R-717), pentane (R-601), 1,1,1,3,3-pentafluoropropane (R-245fa), and water (R-718). These were chosen as benchmarks in this study because they collectively cover a wide range of feasible operating temperatures and chemical families. For each source-sink temperature pair, the refrigerant was fixed to each benchmark fluid and the COP and the VHC were maximized.

RESULTS AND DISCUSSION

Benchmarks

In Table 3, the best of the four benchmark fluids with the highest value of COP is shown for each source-sink temperature pair. Similarly, the best benchmark fluid with VHC as the design objective has also been identified (results shown in SI). The name of the highest-COP benchmark for each source-sink pair is given. Below the name is the optimized value of the objective. In Table 3, pentane dominates at lower source temperatures, being the top benchmark for 6 out of 15 source-sink temperature pairs. At higher temperatures, water emerges as the best benchmark fluid.

Table 3: Best of four benchmark refrigerants for COP at varying source and sink temperatures.

COP		T_{source} (K)				
		340	360	380	400	420
T_{sink} (K)	360	Ammonia **6.99**	–	–	–	–
	380	Pentane **3.35**	R-245fa **5.88**	–	–	–
	400	Pentane **2.19**	Pentane **3.15**	Water **8.56**	–	–
	420	Pentane **1.53**	Pentane **2.02**	Water **5.28**	Water **9.03**	–
	440	No solutions **N/A**	Pentane **1.34**	Water **3.87**	Water **5.55**	Water **9.47**

Case 1: Maximization of VHC

In Table 4, for each source-sink temperature pair, the best-found refrigerant molecule for maximizing the VHC, after applying 3 integer cuts, is shown. The value of the VHC is given in bold in MJ m^{-3}. In brackets next to this, is the percentage change in VHC compared to the benchmark fluid that achieves the highest VHC for a given source-sink temperature. At T_{source} = 360 K, T_{sink} = 380 K, the best-found refrigerant was butadiene with a VHC of 8.03; however, butadiene polymerizes easily, therefore the second-best solution is displayed instead and highlighted with an asterisk.

Typically, for any fixed source temperature, the VHC reduces as the ΔT_{lift} increases. We note that this trend is not followed in Table 4 at T_{source} = 360 K as the second-best solution is reported for ΔT_{lift} = 20 K. The maximum VHC observed was 15.14 at T_{source} = 420 K, T_{sink} = 440 K , the smallest ΔT_{lift} value of 20 K. The minimum was 1.88 at T_{source} = 340 K, T_{sink} = 440 K which is at the largest ΔT_{lift} value of 100 K.

The results indicate that the refrigerant that maximizes the VHC varies with the source-sink temperatures. 7 distinct optimal refrigerants were identified. In 1 out of the 15 tested instances, the VHC value obtained by CAMPD was 57.8% lower than that of ammonia, the best benchmark fluid for that instance. It is worth noting that ammonia was not included in the design

Table 4: Maximization of VHC for case 1 at varying source and sink temperatures.

VHC (MJ m^{-3})		T_{source} (K)				
		340	360	380	400	420
T_{sink} (K)	360	1,1-Difluoroethane **9.78** (-57.8%)	–	–	–	–
	380	1,1,2-Trifluoroethane **5.57** (+104.8%)	1,2-Difluoropropane* **3.70** (-24.9%)	–	–	–
	400	3,3-Difluoropropene **3.98** (+323.4%)	3,3-Difluoropropene **6.26** (+247.8%)	3,3-Difluoropropene **9.59** (+185.4%)	–	–
	420	1,1-Difluoroethanamine **2.84** (+323.9%)	1-Chloro-2,2-difluoroethane **3.72** (+188.4%)	Methanol **6.39** (+163.0%)	Methanol **10.55** (+133.9%)	–
	440	1-Chloro-2,2-difluoroethane **1.88** (N/A)	Methanol **3.40** (+286.4%)	Methanol **5.89** (+145.4%)	Methanol **9.66** (+137.9%)	Methanol **15.14** (+132.6%)

space of the CAMPD problem and, thus, could not have been found as a solution. For 12 out of 15 instances, the use of CAMPD resulted in large improvements of VHC over the best of the benchmark fluids. 1,1-Difluoroethanamine yielded a 323.9% increase in VHC when compared with pentane (R-601), the best benchmark fluid at $T_{source} = 340$ K and $\Delta T_{lift} = 80$ K.

All of the identified refrigerants were novel. One olefin, 3,3-difluoropropene, was found in this case study. 3,3-Difluoropropene belongs to the hydrofluoroolefin family of refrigerants, several of which have been examined in HPs, due to their high COPs, low GWPs and low flammability. One novel oxygenated refrigerant, methanol, was identified; methanol is found to be an excellent candidate in other case studies as well. The novel hydrochlorofluorocarbon (HCFC) 1-chloro-2,2-difluoroethane was also identified; HCFCs have been widely used as refrigerants.

The average pressure ratio across all 15 instances was 6.45 with a maximum pressure ratio of 17.72. Most compressor types are able to achieve pressure ratios up to 10, and screw compressors can achieve pressure ratios up to 20 [20]. ΔT_{super} was negligible for all instances; however, ΔT_{sub} was consistently high, reaching a maximum of 40.37 K at $T_{source} = 380$ K, $T_{sink} = 420$ K. These results are all expected because condenser pressures are increased in order to maximize the energy that is delivered by unit volume of refrigerant. We planned to add 3 integer cuts to generate designs for each of the 15 source-sink temperature pairs shown in Table 4, resulting in a total of 60 optimizations. However, for 2 of the solutions in Table 4, optimizations failed to converge after the addition of the first and second integer cuts respectively, and thus further cuts were not added. The 57 optimizations took an average of 702.2 s, with a maximum of 7138.1 s and minimum of 13.5 s.

Case 2: Maximization of COP

In Table 5, the refrigerant that maximizes the COP for each source-sink temperature pair is shown. This refrigerant corresponds to the best-found solution after 3 integer cuts. The value of the COP achieved by the refrigerant is shown in bold. In brackets, the percentage change of this COP value with respect to the COP of the best benchmark fluid for that source-sink temperature pair is shown.

The COP values in Table 5 illustrate the dependence of the performance of the HP on source-sink temperatures and temperature lifts. For each T_{source}, the COP decreases as T_{sink} increases, i.e. as ΔT_{lift} increases. For any fixed value of ΔT_{lift}, higher COPs are obtained when T_{sink} is higher. The maximum obtained COP is 9.46 by the refrigerant 2-fluoroethanol at $T_{source} = 420$ K, $T_{sink} = 440$ K. Fluorinated alcohols are not common refrigerants.

The results demonstrate that the choice of objective function strongly impacts designs, including the choice of optimal refrigerant. For 14 out of the 15 source-sink pairs that are tested, the refrigerant that maximizes the COP (Table 5) is distinct from the refrigerant that maximizes the VHC (Table 4).

The results indicate the refrigerant that maximizes the COP varies with source-sink temperatures. For the 15 total source-sink pairs that are tested, 5 distinct optimal

Table 5: Maximization of COP for case 2 at varying source and sink temperatures.

COP		T_{source} (K)				
		340	360	380	400	420
T_{sink} (K)	360	3-Fluoropropene **7.81** (+11.7%)	–	–	–	–
	380	Methanol **4.81** (+43.6%)	Methanol **8.16** (+38.8%)	–	–	–
	400	Methanol **3.52** (+60.7%)	3-Fluoropropene **4.98** (+58.1%)	Fluoromethanamine **8.73** (+2.0%)	–	–
	420	3-Fluoropropene **2.72** (+77.8%)	Ethanol **3.64** (+80.2%)	Fluoromethanamine **5.39** (+2.1%)	Fluoromethanamine **9.11** (+0.9%)	–
	440	3-Fluoropropene **2.22** (N/A)	Methanol **2.84** (+111.9%)	Ethanol **3.70** (-4.4%)	Fluoromethanamine **5.59** (+0.7%)	2-Fluoroethanol **9.46** (-0.1%)

refrigerants were identified. 3-Fluoropropene (also known as allyl fluoride) was a common solution in case 2, appearing as the best-found solution for 4 out of 15 temperature pairs. This is a known compound but has no documented use as a HP refrigerant. A novel fluorinated amine molecule, fluoromethanamine, was identified in this case study.

In case 2, improvements to the COP have been observed for 12 out of 15 source-sink pairs when compared with the best benchmark, illustrating the benefits of selecting a refrigerant tailored to the application. At $T_{source} = 360$ K, $T_{sink} = 440$ K, a COP improvement of 111.9% was obtained by choosing methanol as the refrigerant. Screening studies [6] and [8] which examined a small set of molecules have also found methanol to be a promising refrigerant. It is highly promising that the CAMPD framework which is using optimization to implicitly search through a large design space with $2 * 11^{19}$ possible combinations of groups has also been able to identify this high-performance fluid.

In case 2, the pressure ratio increased as ΔT_{lift} increased. The maximum pressure ratio observed was 14.5 at the maximum ΔT_{lift} of 100 K, for 3-fluoropropene. The minimum pressure ratio was 2.15 observed at $\Delta T_{lift} =$ 20 K and $T_{source} = 400$ K. The pressure ratios were all below 20 and were below 10 for 12 out of the 15 source-sink pairs. Pressure ratios above ten were only observed at high values of ΔT_{lift} of 80 K and 100 K. This highlights that the design of high temperature lift HP cycles is indeed more challenging than cycles with low ΔT_{lift} and necessitates the addition of equipment-related constraints. ΔT_{super} and ΔT_{sub} remained negligible for all results in case 2. Case 2 had an average total solve time of 36.3 s over a total of 60 optimizations, with a maximum solve time of 165.0 s and a minimum of 12.0 s.

Case 3: Maximizing COP with GWP, ODP, & Design Space Constraints

In Table 6, the best low-GWP and zero-ODP refrigerant that is found for each source-sink temperature pair is shown. GWP values are constrained to be below 150 in accordance with environmental regulations [5]. The COP value is shown in bold. In brackets, the percentage change of this COP value with respect to the best benchmark fluid for that source-sink temperature pair is shown. The refrigerant design space is much more restricted in case 3. Chlorinated molecules are removed from the search space to obtain zero ODP refrigerants; fluorinated molecules are disallowed as several of these may be phased out; and we also exclude nitrogenated molecules.

For case 3 all of the obtained solutions are oxygenated molecules, as shown in Table 6. Ethanol was found to be the best-fit low-GWP refrigerant in 9 out of 15 instances. Methanol was found to be the top solution for 5 out of 15 points. It is not currently used in vapour-compression HPs but several computational studies ([6], [8]) have indicated methanol to be a high-performance refrigerant for HPs. [6] Found methanol to be a high performing refrigerant for high temperature HPs, for COP at condensing temperatures of around 200 °C. [8] Found methanol to be a top performing subcritical HP refrigerant alongside acetone and ethanol, the other

optimal refrigerants identified in this case study. While methanol is not yet used in industrial vapour-compression HPs, it is likely to be widely used given its superior heat transfer properties and low viscosity. It is also used in adsorption HPs, and organic Rankine cycles.

Table 6: Maximization of COP for case 3 at varying source and sink temperatures.

COP		T_{source} (K)				
		340	360	380	400	420
T_{sink} (K)	360	Acetone **7.79** (+11.4%)	–	–	–	–
	380	Methanol **4.81** (+43.6%)	Ethanol **8.22** (+39.8%)	–	–	–
	400	Methanol **3.52** (+60.7%)	Ethanol **5.04** (+60.0%)	Ethanol **8.55** (-0.1%)	–	–
	420	Methanol **2.79** (+82.4%)	Ethanol **3.64** (+80.2%)	Ethanol **5.18** (-1.9%)	Ethanol **9.08** (+0.6%)	–
	440	Methanol* **2.31** (N/A)	Methanol **2.84** (+111.9%)	Ethanol **3.70** (-4.4%)	Ethanol **5.54** (-0.2%)	Ethanol **9.41** (-0.6%)

While acetone, ethanol, and methanol are all stable compounds with several industrial uses, their chief drawback is their flammability. These flammable refrigerants may be used in industry and even homes with appropriate controls and safety features.

Interestingly, imposing constraints on GWP, ODP and restricting the molecular design space led to no reductions in COP on average; instead, a small improvement in COP of 0.04% on average was observed. COP in case 3 differed from case 2 by -3.9% to +4.1%.. For the third integer cut at $T_{source} = 340$ K and $T_{sink} = 440$ K, the optimization failed to converge to a solution after 12 hours, so the reported result (marked with an asterisk) is the best of 2 integer cuts. Across all 59 converged optimizations in case study 3, the average solve time was 18.6 s, with a maximum of 90.3 s and a minimum of 7.2 s.

CONCLUSIONS

This paper takes a multi-scale process systems engineering approach to the design of industrial HPs leveraging process modelling, equations of state, and optimization. Industrial HPs with high COPs and high VHCs were designed in this work for a range of source-sink temperature pairs, demonstrating their potential to decarbonise heat in the chemical industry. New stability constraints were introduced into the CAMPD formulation for the first time to obtain meaningful solutions (see SI). In addition, low-GWP and zero-ODP refrigerants that maximize the COP were designed. The results of case studies 1 and 2 illustrate that there is no single universal optimal refrigerant for all use cases: the optimal refrigerant and process conditions vary with source and sink temperatures, objectives, and design constraints. The results highlight the intrinsic link between refrigerant and heat-pump performance. COP was maximized in cases 2 and 3 in an average of 27.5 s. The optimization implicitly searched through a vast molecular design space with $2 * 11^{19}$ combinations of groups to identify high-performing refrigerants for each source-sink pair. Refrigerants identified in this work include known fluids that other authors have found to be promising and a few novel molecules. First-order GCMs were used to predict physical properties in this work, which may lead to lower-accuracy solutions. Validation steps that consider structural information of the molecule are necessary. For case study 3, we used literature data where available to certify that the identified known molecules indeed had low GWP and zero-ODP. Compressor ratios and discharge temperatures were not limited in this study, and this will be the subject of future work.

DIGITAL SUPPLEMENTARY MATERIAL

The digital supplementary material includes the process constraints, VHC benchmarks, and initial values for decision variables. This can be found at the following link: https://psecommunity.org/LAPSE:2026.0039

REFERENCES

1. International Energy Agency, *Renewables 2023*. IEA Publications, 2023.
2. Thiel GP, Stark AK. To decarbonize industry, we must decarbonize heat. Joule 5:531-550 (2021). https://doi.org/10.1016/j.joule.2020.12.007
3. Marina A, Spoelstra S, Zondag HA, Wemmers AK. An estimation of the european industrial heat pump market potential. Renewable and Sustainable Energy Reviews 139:110545 (2021). https://doi.org/10.1016/j.rser.2020.110545
4. United Nations, The Montreal Protocol on Substances that Deplete the Ozone Layer, Kigali update 2016. Kigali, 2016. doi: 10.4324/9781003597681.
5. European Parliament and Council, 'Regulation (EU) 2024/573 on fluorinated greenhouse gases', *Official Journal of the European Union*. 2024. [Online]. Available: https://eur-lex.europa.eu/eli/reg/2024/573/oj
6. Zini A, Socci L, Vaccaro G, Rocchetti A, Talluri L.

Working fluid selection for high-temperature heat pumps: a comprehensive evaluation. Energies 17:1556 (2024). https://doi.org/10.3390/en17071556
7. Abedini H, Vieren E, Demeester T, Beyne W, Lecompte S, Quoilin S, Arteconi A. A comprehensive analysis of binary mixtures as working fluid in high temperature heat pumps. Energy Conversion and Management 277:116652 (2023). https://doi.org/10.1016/j.enconman.2022.116652
8. Vieren E, Demeester T, Beyne W, Arteconi A, De Paepe M, Lecompte S. The thermodynamic potential of high-temperature transcritical heat pump cycles for industrial processes with large temperature glides. Applied Thermal Engineering 234:121197 (2023). https://doi.org/10.1016/j.applthermaleng.2023.121197
9. Neumaier L, Roskosch D, Schilling J, Bauer G, Gross J, Bardow A. Refrigerant selection for heat pumps: the compressor makes the difference. Energy Tech 11: (2023). https://doi.org/10.1002/ente.202201403
10. Papaioannou V, Lafitte T, Avendaño C, Adjiman CS, Jackson G, Müller EA, Galindo A. Group contribution methodology based on the statistical associating fluid theory for heteronuclear molecules formed from mie segments. The Journal of Chemical Physics 140: (2014). https://doi.org/10.1063/1.4851455
11. Bowskill DH, Tropp UE, Gopinath S, Jackson G, Galindo A, Adjiman CS. Beyond a heuristic analysis: integration of process and working-fluid design for organic rankine cycles. Mol. Syst. Des. Eng. 5:493-510 (2020). https://doi.org/10.1039/c9me00089e
12. J. Santiuste Martínez, 'Development of a SAFT-γ Mie group contribution approach to modelling working fluids and its application in the computer aided molecular and process design of ORCs', Jul. 2020, [Online]. Available: https://uvadoc.uva.es/bitstream/handle/10324/42747/TFM-I-1655.pdf
13. Hukkerikar AS, Sarup B, Ten Kate A, Abildskov J, Sin G, Gani R. Group-contribution+ (GC+) based estimation of properties of pure components: improved property estimation and uncertainty analysis. Fluid Phase Equilibria 321:25-43 (2012). https://doi.org/10.1016/j.fluid.2012.02.010
14. JOBACK KG, REID RC. ESTIMATION OF PURE-COMPONENT PROPERTIES FROM GROUP-CONTRIBUTIONS. Chemical Engineering Communications 57:233-243 (2007). https://doi.org/10.1080/00986448708960487
15. Y. Nannoolal, J. Rarey, and D. Ramjugernath, 'Estimation of pure component properties Part 2. Estimation of critical property data by group contribution'.
16. Hukkerikar AS, Kalakul S, Sarup B, Young DM, Sin G, Gani R. Estimation of environment-related properties of chemicals for design of sustainable processes: development of group-contribution⁺ (gc⁺) property models and uncertainty analysis. J. Chem. Inf. Model. 52:2823-2839 (2012). https://doi.org/10.1021/ci300350r
17. Hodnebrog Ø, Aamaas B, Fuglestvedt JS, Marston G, Myhre G, Nielsen CJ, Sandstad M, Shine KP, Wallington TJ. Updated global warming potentials and radiative efficiencies of halocarbons and other weak atmospheric absorbers. Reviews of Geophysics 58: (2020). https://doi.org/10.1029/2019rg000691
18. Samudra AP, Sahinidis NV. Optimization-based framework for computer-aided molecular design. AIChE Journal 59:3686-3701 (2013). https://doi.org/10.1002/aic.14112
19. S. Gopinath, 'Molecular design, process design and process synthesis of separation systems', Imperial College London, 2018.
20. B. Zühlsdorf *et al.*, 'High Temperature Heat Pumps, Task 1 - Technologies', Danish Technological Institute, HPT-AN58-2, Aug. 2023. Accessed: Jan. 30, 2026. [Online]. Available: https://heatpumpingtechnologies.org/content/uploads/sites/70/2023/09/annex-58-task-1-technologies-task-report.pdf
21. Wasik DO, Lasala S, Herbinet O, Samukov K, Calero S, Vlugt TJH. Multiscale modeling of dimerization thermodynamics of formic acid. Fluid Phase Equilibria 594:114356 (2025). https://doi.org/10.1016/j.fluid.2025.114356

© 2026 by the authors. Licensed to PSEcommunity.org and PSE Press. This is an open access article under the creative commons CC-BY-SA licensing terms. Credit must be given to creator and adaptations must be shared under the same terms. See https://creativecommons.org/licenses/by-sa/4.0/